

See discussions, stats, and author profiles for this publication at: <https://www.researchgate.net/publication/265056115>

# Tuning Emission Colors from Blue to Green in Polymeric Light-Emitting Diodes Fabricated using Polyfluorene Blends

ARTICLE *in* THE JOURNAL OF PHYSICAL CHEMISTRY A · AUGUST 2014

Impact Factor: 2.69 · DOI: 10.1021/jp503819u · Source: PubMed

---

CITATION

1

---

READS

17

4 AUTHORS, INCLUDING:



José Carlos Germino

University of Campinas

7 PUBLICATIONS 3 CITATIONS

SEE PROFILE



T.D.Z. Atvars

University of Campinas

139 PUBLICATIONS 1,460 CITATIONS

SEE PROFILE

# Tuning Emission Colors from Blue to Green in Polymeric Light-Emitting Diodes Fabricated using Polyfluorene Blends

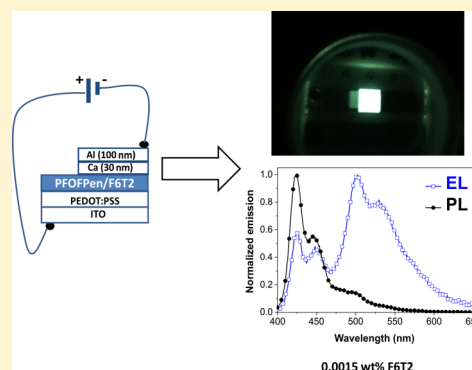
Fernando Júnior Quites,<sup>†</sup> Gregório Couto Faria,<sup>‡</sup> José Carlos Germino,<sup>†</sup>  
and Teresa Dib Zambon Atvars<sup>\*,†</sup>

<sup>†</sup>Chemistry Institute, State University of Campinas, POB. 6154, Campinas, 13084-971 SP, Brazil

<sup>‡</sup>Instituto de Física de São Carlos, University of São Paulo, POB. 369, São Carlos, 13560-970 SP, Brazil

## S Supporting Information

**ABSTRACT:** The photo- and electroluminescent properties of single-layer two-component blends composed of one blue emitter polymer and one green emitter polymer were studied. The blue emitter, poly[(9,9-dioctylfluorenyl-2,7-diyl)-*alt-co*-(9,9-di-*{S'}*-pentanyl)-fluorenyl-2,7-diyl)] (PFOFPe), was used as the matrix, and the green emitter, poly[(9,9-dihexylfluorenyl-2,7-diyl)-*alt-co*-(bithiophene)] (F6T2), was used as the guest. The F6T2 content in the blends varied from 0.0075 wt % to 2.4 wt %. Remarkable differences were observed between the electroluminescent (EL) and photoluminescent (PL) spectra of these blends, which indicated that the mechanism for excited-state generation in the former process had a higher efficiency in the aggregated phase than in the nonaggregated phase. Blending these two polymers gradually tuned the emission color from blue (PFOFPe and blends with <0.75 wt % F6T2) to green (F6T2 and blends with >0.75 wt % F6T2). The photophysical processes involved in both EL and PL emission are also discussed.



## 1. INTRODUCTION

Since the discovery of polymer light-emitting diodes (PLEDs),<sup>1</sup> efforts have been directed toward developing new materials, architectures, and fabrication processes for the creation of devices with improved performances.<sup>2–10</sup> PLED is the acronym that refers to a light-emitting diode that uses conjugated polymers as the active medium. This nomenclature is used to differentiate these materials from inorganic electroluminescent diodes (LEDs). When small molecules of coordination compounds are used as the active medium, the appropriate acronym is OLED.

The fabrication of colored light-emitting diodes (LEDs) using organic molecules, phosphors, or polymers is often guided by the CIE coordinates ( $x$ ,  $y$ ) defined by the Commission Internationale de l'Éclairage, which can be used to specify the emission color of such devices. Different colors can be achieved by preparing different combinations of fluorescent or phosphorescent compounds,<sup>5–21</sup> building multi-layer systems in which each layer is composed of molecules or polymers as the active medium,<sup>4,11,13,22</sup> combining multiple layers in a tandem diode architecture,<sup>17</sup> using a single polymer with multiple functional groups,<sup>3,5,18</sup> using mixtures of polymers with small phosphorescent<sup>19</sup> or fluorescent<sup>5,20</sup> molecules (host/guest systems), quantum dots,<sup>22,26</sup> or nano-rods/nanotubes,<sup>10,23</sup> using systems with excimer or exciplex emissions,<sup>24,25</sup> using systems that form exciplexes in bilayer structures,<sup>4,6</sup> or preparing blends with conjugated polymers.<sup>7,11,15,16,26–32</sup> The use of polymer blends represents a relatively inexpensive approach to the preparation of novel

polymeric electroluminescent (EL) diodes with acceptable performances.<sup>5,6,8</sup>

Furthermore, after the active materials are chosen, the diode architecture must be optimized to improve the device performance in terms of light output, turn-on voltage, whiteness, and brightness properties.<sup>5,6,13,30</sup> Polymers have emerged as a promising technology for large-area diodes and for flexible diodes,<sup>5,33,34</sup> which can be processed using solution-based and conventional printing techniques (e.g., roll-to-roll or inkjet techniques).<sup>6,7,33,34</sup> In this regard, PLEDs are an interesting target because of their ability to be easily processed using solution-based methods.<sup>26,33</sup>

Although all of the above-mentioned types of multicolored diodes have been successfully reported in the literature, certain difficulties are associated with each one. For example, in several cases, the mixing of polymers has been found to generate immiscible systems that undergo phase separation.<sup>35</sup> The phase-separation process in polymer blends results in a complex and metastable nonequibrated morphology that is strongly dependent on the composition and methodology of the blend preparation.<sup>32,35–37</sup> Thus, the reproducibility of the device performance is highly problematic.<sup>38,39</sup> Although this particular difficulty is always present, the performance of devices that use

**Special Issue:** Current Topics in Photochemistry

**Received:** April 18, 2014

**Revised:** August 11, 2014

**Published:** August 16, 2014

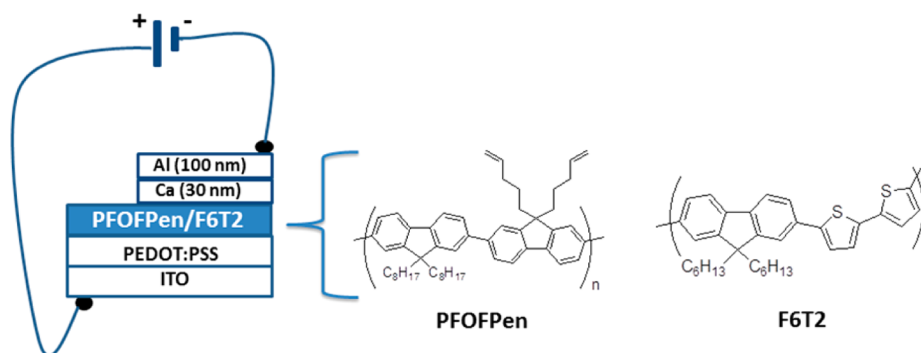


**Figure 1.** Configuration of the polymer light-emitting diodes, ITO/PEDOT:PSS/polymer/Ca/Al, and the chemical structures of the components of the polymeric emissive layer. The polymer consists of PFOFPe, F6T2, or a blend thereof.

polymer blends as the active media is often improved by the presence of bulk heterojunctions that can facilitate the diffusion of charge carriers.<sup>39–43</sup>

Furthermore, the blending of materials also requires additional precautions in the choice of the multicolored components because of the possibility of nonradiative energy-transfer processes when a component that emits at a lower energy also absorbs in the spectral range of emission of another component that emits at a higher energy.<sup>44</sup> This nonradiative resonant energy transfer process is known as the Förster energy transfer mechanism<sup>45</sup> (FRET, in IUPAC terminology<sup>46</sup>), and it may quench or decrease the intensity of the higher energy emission band. When the FRET process is very efficient, the higher energy component of the emission is eliminated. Nevertheless, when a judicious concentration of the lower energy component is used, both color tuning and an increase in the luminous performance can be achieved simultaneously.

In summary, an effective strategy for the color tuning light emitting diodes requires the use of low-cost polymers that can be processed using common techniques, exhibit stable morphologies after mixing, and can be combined into materials that emit energy over a wide spectral range. To facilitate the development of such a streamlined approach, we report the performance of single-layer diodes whose emission color can be tuned by modifying the composition of the polymer blend. These diodes have the following configuration: ITO/PEDOT:PSS/(polymer blend)/Ca/Al, where the polymer blend is composed of a mixture of a blue-emitting component, poly[(9,9-dioctylfluorenyl-2,7-diyl)-*alt-co*-(9,9-di-{*S'*-pentanyl}-fluorenyl-2,7-diyl)] (PFOFPe) and a green-emitting component, poly[(9,9-dihexylfluorenyl-2,7-diyl)-*alt-co*-(bithiophene)] (F6T2); the chemical structures of the two components and the diode configuration are illustrated in Figure 1. We also discuss the differences between the PL and EL emissions in blends of PFOFPe and F6T2 in thin films with the same proportions as those used in the diodes.

## 2. EXPERIMENTAL SECTION

**2.1. Materials.** Poly[(9,9-dioctylfluorenyl-2,7-diyl)-*alt-co*-(9,9-di-{*S'*-pentanyl}-fluorenyl-2,7-diyl)] (PFOFPe) (ADS150BE) ( $M_w$  = 6000 g/mol and polydispersity = 2.3) and poly[(9,9-dihexylfluorenyl-2,7-diyl)-*alt-co*-(bithiophene)] (F6T2) (ADS2006P) ( $M_w$  = 20 000 g/mol and polydispersity = 2.2) were purchased from American Dye Source (Quebec, Canada) and used as received. Poly(*N*-vinyl carbazole) (PVK) was purchased from Sigma-Aldrich,  $M_w$  = 110 000 g/mol. THF was purchased from Tedia (Rio de Janeiro, Brazil) at

HPLC/Spectro grade and was distilled before use. The concentrations of the polymer solutions in THF were calculated based on the molar masses of the monomers and were represented as wt % (percentage by weight) of F6T2. Poly(ethylene dioxathiophene):poly(4-styrenesulfonate) (PEDOT:PSS) was purchased from Baytron P CH 8000 (Bayer AG, Germany).

Films of PFOFPe or F6T2 were deposited by spin-coating a THF solution with a polymer concentration of 5.0 mg mL<sup>−1</sup> onto a PEDOT:PSS surface supported on an ITO/glass substrate. Films of the PFOFPe/F6T2 blends were deposited by mixing appropriate volumes of the THF solutions of each polymer, with concentrations of 5.0 mg mL<sup>−1</sup> to yield films of various molar compositions: 0.0015%, 0.0075%, 0.075%, 0.37%, 0.75%, and 2.4% by weight of F6T2. These solutions were maintained at room temperature in the dark for 1 week for complete polymer dissolution. The mixtures were then spin-coated (1500 rpm) onto a clean ITO/glass substrate (see below for further details).

**2.2. Methods.** <sup>13</sup>C NMR spectra of the PFOFPe polymer was recorded on an Advanced 400 spectrometer in deuterated chloroform solution at ambient temperature with tetramethylsilane as the internal standard.

Sample for Fourier-transform infrared (FTIR) spectroscopy measurement was prepared by PFOFPe dispersed in anhydrous KBr pellets at a concentration of 0.5 wt %. FTIR spectrum was then recorded from 400 to 4000 cm<sup>−1</sup> using a Nicolet 6700 spectrometer with a resolution of 4 cm<sup>−1</sup>.

The steady-state emission spectra of the polymer films were acquired using a Cary Eclipse spectrofluorimeter in the 390–700 nm spectral range with an excitation wavelength of  $\lambda_{exc}$  = 370 nm. The PL spectrum was corrected for lamp intensity and detector response. The films were oriented in a back-face configuration and were supported by a homemade optical support.

Fluorescence decays were recorded using a time-correlated single photon counting technique in an Edinburg Analytical Instruments FL 900 spectrofluorimeter with a MCP-PMT (Hamamatsu R3809U-50). A pulsed diode with  $\lambda_{exc}$  = 370 nm (model EPL-370, bandwidth of 5 nm, 77 ps) was used for the PFOFPe excitation, and the decay signal was collected at  $\lambda_{em}$  = 420 nm (peak position). The instrument response was determined using Ludox samples and was deconvoluted from the sample signal using the software provided by Edinburg. For the lifetime determination, data acquisition was allowed to continue until at least 10 000 counts had accumulated in the peak channel. The emission decays were analyzed using

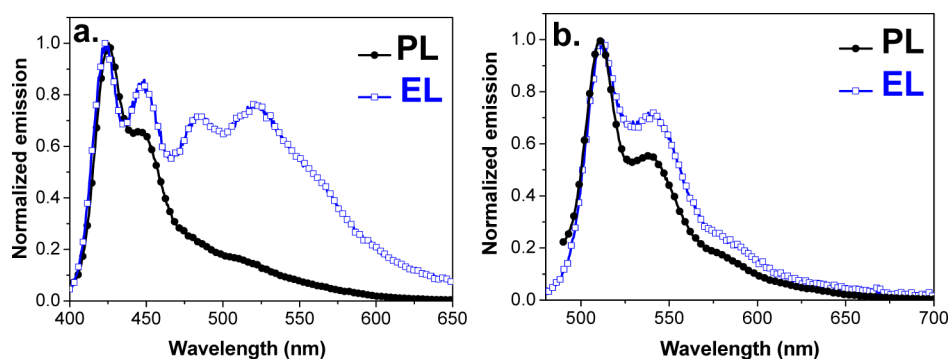


**Figure 2.** Normalized PL and EL Spectra of the (a) PFOFPe and (b) F6T2 films in diodes with the configuration ITO/PEDOT:PSS(30 nm)/polymer/Ca(30 nm)/Al(100 nm).

exponential functions, as previously described.<sup>16,18,30</sup> Time-resolved emission spectra (TRES) were recorded using a pulsed diode with  $\lambda_{\text{exc}} = 370$  and pulsed diode lasers with  $\lambda_{\text{exc}} = 404$  nm (model EPL-404, bandwidth of 5 nm, 70 ps) for the excitation of the blue- and green-emitting components. For  $\lambda_{\text{exc}} = 370$  nm, the decays were recorded over an emission range of  $\lambda_{\text{em}} = 420$  to 600 nm, whereas for  $\lambda_{\text{exc}} = 440$  nm, the decays were recorded over an emission range of  $\lambda_{\text{em}} = 470$  to 600 nm. Both data streams were partitioned at intervals of 10 nm. Delays of 0 to 6.4 ns after the excitation pulses were used to generate the TRES spectral plots.

A potentiostat/galvanostatic PAR 273A was used for the electrochemical characterization of the frontier orbital energies of both PFOFPe and F6T2 polymers. Three electrodes electrochemical cell was used. The working electrode was Pt, the reference one was Ag/Ag<sup>+</sup> in acetonitrile, and the counter electrode was Pt, supporting electrolyte (0.1 mol L<sup>-1</sup> tetrabutylammonium hexafluorophosphate in acetonitrile). The ferrocenium/ferrocene pair was used as the internal standard.

**2.3. Fabrication and Characterization of Light-Emitting Diodes.** For the diode fabrication, an ITO substrate (25  $\Omega/\text{cm}^2$  from Delta Technologies) was initially washed with acetone, 2-propanol, and deionized water in an ultrasonic bath, dried on a hot plate at 130  $^{\circ}\text{C}$  for 10 min, and subsequently treated with UV ozone for 30 min. A 30 nm thick layer of a hole-injection material, PEDOT:PSS, was spin-coated onto the ITO substrate. After this deposition, the PEDOT:PSS film was annealed for 30 min at 110  $^{\circ}\text{C}$ . Subsequently, the polymer (PFOFPe, F6T2, or a blend thereof) was spin-coated using a THF solution (5.0 mg mL<sup>-1</sup>) in a controlled-atmosphere environment, resulting in an 80 nm thick film. After deposition, this system was annealed at 70  $^{\circ}\text{C}$  for 15 min. Finally, thin layers of calcium (30 nm) and aluminum (100 nm) were deposited via thermoevaporation under a vacuum of  $10^{-6}$  mbar in an MBraun Evaporator. The fabricated device was then transported to a glovebox ( $\text{H}_2\text{O}$ ,  $\text{O}_2 < 1$  ppm) for testing. Figure 1 illustrates the architecture of these PLEDs.

The ITO/PEDOT:PSS/polymer/Ca/Al diodes were analyzed with respect to their electrical properties and electro-emission (EL) profiles. For comparison, a diode composed of ITO/PEDOT:PSS/PVK/PFOFPe/Ca/Al, with each layer being deposited in the same way as indicated before. The current–voltage measurements ( $J \times V$ ) were performed using a 2400 Keithley Source Meter. The EL spectra were acquired using a Labsphere Diode Array Spectrometer 2100 connected to a Labsphere System Control 5500. The luminance–voltage

behavior ( $L \times V$ ) was measured using a Keithley 238 current source connected to a photodiode. The samples were stored in a sealed Janis chamber under high vacuum. The CIE coordinates were calculated based on data acquired from the EL or PL emissions using CIE 31 xyz.xls.

### 3. RESULTS AND DISCUSSION

**3.1. EL Properties of PFOFPe and F6T2 Diodes.** Figure 2 presents a comparison of the PL and EL spectra of each polymer (PFOFPe and F6T2). The PFOFPe EL spectrum exhibits bands in two spectral regions: a band at higher energy with a vibronic structure at 424 nm (zero phonon) and 448 nm (first replica) and a band in a lower-lying region at approximately 500–580 nm, which has a very low relative intensity in the PL spectrum. The relative intensity of this lower-energy band is highly pronounced in the EL spectrum compared with the PL spectrum (Figure 2a). The EL emission presented CIE coordinates of (0.23, 0.30), corresponding to a blue-greenish color (see Figure 4). Additional details regarding these PL and EL emissions are discussed below. For F6T2, both the PL and EL spectra, presented in Figure 2b, exhibit similar profiles with bands at 511 nm (zero phonon), 540 nm (0–1 band), and 580 nm (0–2 band).

Table 1 summarizes the electrical properties of these two diodes; the turn-on voltage, maximum brightness (at 8 V), and

**Table 1.** Some EL Properties and the CIE Coordinates for Diodes with the Structure ITO/PEDOT:PSS(30 nm)/Polymer/Ca(30 nm)/Al(100 nm), Where the Polymer is PFOFPe or F6T2

sample	$\lambda_{\text{EL,max}}$ (nm)	$V_{\text{on}}$ (V)	$L_{\text{max}}$ ( $\text{cd m}^{-2}$ )	$\text{CE}_{\text{max}}$ ( $\text{cd A}^{-1}$ )	CIE (x, y)
PFOFPe	424 and 522	4.0	124	344	0.23, 0.30
F6T2	512	2.6	226	383	0.29, 0.63

$\lambda_{\text{max}}$  = EL peak,  $V_{\text{on}}$  = turn-on voltage,  $L_{\text{max}}$  = maximum luminance, and  $\text{CE}_{\text{max}}$  = maximum current efficiency. CIE coordinates were obtained at 8.0 V.

maximum luminous efficiency of the polymers are, respectively, 3.6 V, 140  $\text{cd m}^{-2}$ , and 0.40  $\text{cd A}^{-1}$  for PFOFPe and 2.3 V, 240  $\text{cd m}^{-2}$ , and 0.62  $\text{cd A}^{-1}$  for F6T2, as obtained from Figure 3. It is clear that F6T2 has a lower turn-on voltage, a higher maximum brightness, and a higher maximum luminous efficiency than PFOFPe. The CIE coordinates for the EL emissions of PFOFPe [(0.23, 0.30), blue region] and F6T2 [(0.29, 0.63), green region] are indicated on the CIE



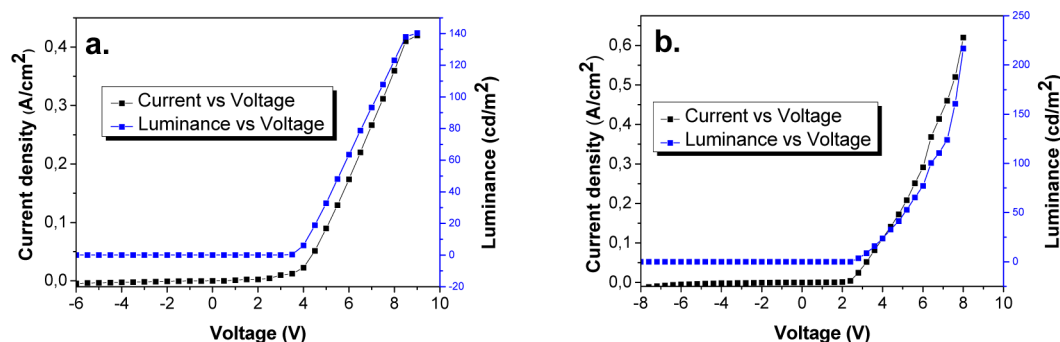


**Figure 3.** Some electrical properties of diodes fabricated using (a) PFOFPe and (b) F6T2 polymers. Diode configuration: ITO/PEDOT:PSS(30 nm)/polymer/Ca(30 nm)/Al(100 nm).

chromaticity diagram in Figure 4 by the numbers 1 and 8, respectively.

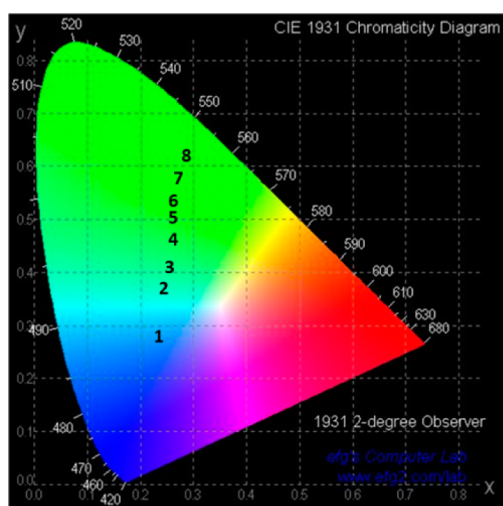


**Figure 4.** CIE diagram on which the coordinates of the EL emission of diodes with the structure ITO/PEDOT:PSS(30 nm)/(polymer or blends)/Ca(30 nm)/Al(100 nm) are indicated, where PFOFPe (1), F6T2 (8), and for blends the composition are 0.0015 wt % (2), 0.0075 wt % (3), 0.075 wt % (4), 0.37 wt % (5), 0.75 wt % (6), and 2.4 wt % (7).

With regard to the PL and EL of PFOFPe, some additional experiments are required to explain such differences. For example, there is a consensus in the literature that the higher-energy band is due to chain segments in the isolated form, whereas the assignment of this green emission of polyfluorenes is controversial (see the discussion about PL of PFOFPe for details of this assignment). Some authors propose that this band is due to structural defects such as the presence of fluorenone moieties.<sup>53–55</sup> Nevertheless, there are also results claiming that this green emission is due to the presence of aggregates.<sup>30–32,39,48–51</sup> Others claimed that the presence of fluorenone groups are emitting in the green when they are locally associated either forming aggregates or excimers.<sup>56–62</sup> Because of these controversial assignments, we performed a series of experiments as an attempt to understand the photophysical behavior of the PFOFPe. In this topic the EL experiments are described and later the PL experiments are presented.

There are some authors also claimed that the fluorenone groups appear after the diode operation due to the polyfluorene

oxidation.<sup>53</sup> This reaction is more evident for higher bias. Thus, we recorded the EL emission spectra in three voltages: 4, 5, and 7 V, and the emission profile is virtually the same (Figure 5). Then the conclusion from these data is that if fluorenone is present, it has not been formed during the diode operation.

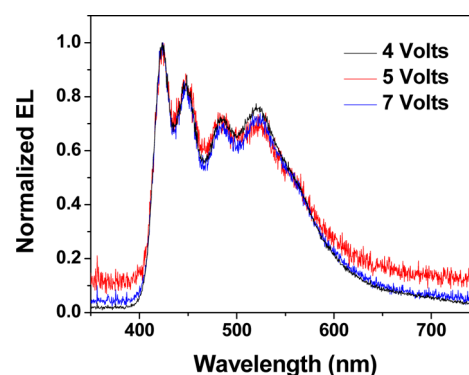


**Figure 5.** EL spectra of the PFOFPe diode in different voltages.

To add new insights for the presence of aggregates, other experiments were performed. It is well-known that polyfluorenes may be disaggregated when diluted in polymer blends<sup>32,63</sup> or when intercalated in some substrates.<sup>64</sup> No green emission was observed under these conditions. Then, taking into account that blending the polyfluorene with other polymers may induce disaggregation of the polyfluorene chains, an EL diode using polyvinylcarbazole (PVK) and PFOFPe was prepared according to the configuration: ITO/PEDOT:PSS/PVK/PFOFPe/Ca/Al. In this diode, a PVK layer (60 nm) from a THF solution (5 mg/mL) was spin-coated on the ITO/PEDOT:PSS substrate. Subsequently, the PFOFPe layer was spin-coated on the ITO/PEDOT:PSS/PVK substrate from a THF solution (5 mg/mL). Because the THF is a good solvent for both, the PVK and the PFOFPe, chain interpenetration of these two polymers should be expected, decreasing the PFOFPe aggregation. Further, because these layers are heated for their thermal relaxation, additional chain interpenetration was expected. The EL spectra of both diodes were compared in Figure 6. Clearly, the green emission intensity is strongly reduced in the presence of PVK, supporting the hypothesis that it is due to aggregates.

To explain these differences between the EL and the PL of the PFOFPe, one might consider the pathways involved in each of these processes that lead to the formation of electronic excited states via photoabsorption (a radiative process induced

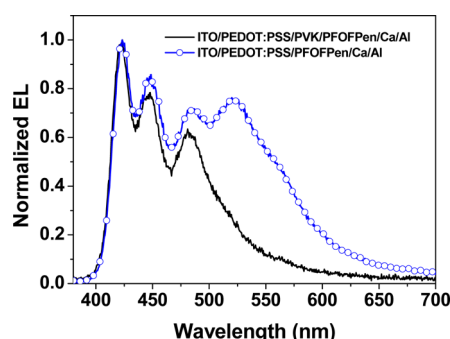


**Figure 6.** Comparison between the EL spectra of the PFOFPe in two diodes: ITO/PEDOT:PSS/PVK/PFOFPe/Ca/Al and ITO/PEDOT:PSS/PFOFPe/Ca/Al.

by photon irradiation) or via charge recombination (a process induced by charge injection). In the former case, the lower-lying PL emission is very weak relative to that at higher energy, which is, among others, due to two reasons: the aggregate population in the electronic excited state is very low and also the PL quantum yield is very low; usually fluorenone emission has low intensity.<sup>60</sup> In general, aggregate emission also has a lower PL quantum yield,<sup>52</sup> which means that one might not expect high-intensity emission from these species. In the particular case of polyfluorenes, the higher-energy emission arises from isolated chain segments, and the lower-energy emission arises from interchain aggregates; the latter type of emission is typically very low.<sup>16,32,49</sup> Because two PL bands are apparent, one might suppose that this polymer matrix is composed predominantly of an amorphous phase with isolated chain segments with some concentration of more ordered interchain aggregates.<sup>47–51</sup>

The mechanism of exciton formation in the EL process is different: it arises from charge recombination (hole and electron injections), which forms an exciton that decays radiatively. In a heterogeneous sample, such as a polymer matrix composed of isolated chain segments and interchain aggregated domains, the charge-recombination efficiencies in these two types of domains could be quite different. For example, it has been demonstrated that charge recombination occurs with higher efficiency near aggregates than in isolated chain domains.<sup>42,43</sup> Thus, as in the case of PL, the higher- and lower-energy EL emissions indicate that there are two emitting species: the excitons of isolated chain segments and those of aggregates. Because the quantum efficiency of the emission of isolated chains in conjugated polymers may be much higher than that of aggregates,<sup>48,52</sup> the higher EL intensity of the aggregates in the PFOFPe diode must be a consequence of very efficient charge recombination in this aggregated phase. The greater the efficiency of exciton generation, the higher the population and its emission intensity might be.

Therefore, as noted in Figure 2a, the remarkable differences in the relative intensities of the EL and PL spectra of the PFOFPe polymer, particularly in the lower-energy spectral region, may be attributed to the presence of fluorenone defects but can equally be attributed to aggregates.<sup>56–60,62–64</sup> This preferential emission can be explained by the relative ordering of the energy levels since, for example, both the HOMO (5.67 eV) and LUMO (3.14 eV) levels of the fluorenone are lying within the band gap of the polyfluorenes (see Figure 10 below).<sup>65</sup> Thus, efficient charge injection processes favor the exciton formation in the fluorenone moieties and may result in

higher relative EL intensity even though the amount of these groups is very low. Nevertheless, the band gap of the aggregates also lies within the polyfluorene band gap, and again, the green emission has higher intensity.

**3.2. PL Properties of PFOFPe-Based Diodes.** The conclusions of the data presented earlier indicate that the PFOFPe itself is a very complex matrix, with heterogeneities in terms of chain interactions in the solid state, producing consequences either in its photophysical or in its electroluminescent properties. Thus, some additional spectroscopic methodologies were used to give additional support for the presence of fluorenone groups in these samples.

For example, fluorenone groups in polyfluorenes have been characterized by the presence of carbonyl stretching vibrational motion around 1720  $\text{cm}^{-1}$  in the FT-IR spectrum<sup>66–69</sup> and by the chemical shift at  $\delta = 194$  ppm in the  $^{13}\text{C}$  RMN spectrum.<sup>69</sup> In Figures S1 and S2 of the Supporting Information, both spectra are exhibited. In the case of the PFOFPe neither the FTIR nor the RMN bands are present. One possible reason for the absence of these bands is that these two fingerprints of the fluorenone groups require a minimal amount of these structural defects to be detected, and in the present samples, the concentration is below this limit.

To add some additional insights for the correlation between its structural or morphological and photophysical properties, the emission spectrum were measured under dynamical conditions. Initially the PL was recorded using  $\lambda_{\text{exc}} = 370$  nm and collecting the decays at different wavelengths from  $\lambda_{\text{em}} = 420$  to 520 nm; covering the spectral region were both components (isolated chains and aggregated/fluorenone defect are emitting) (see Figure S3 of the Supporting Information). Clearly, the emission decay becomes slower as the emission wavelengths increased. In the emission wavelength range of 420–450 nm, two lifetimes were obtained from the decay fitting: a faster component with  $\tau_1 = 0.31 \pm 0.01$  ns, with a contribution of  $B_1 = 52\%$ , and a slower component,  $\tau_2 = 0.73 \pm 0.03$  ns, with a contribution of  $B_2 = 48\%$ . In this emission range, only the PFOFPe chains are emitting. Therefore, in agreement with the assumption that the biexponential decay are related to the presence of two types of lumophores in this polymer matrix, conferring a microheterogeneous distribution of environments around them, one may assume that there are some more isolated chain segments emitting at higher energy, with a lifetime of 0.73 ns similar to that in diluted solutions of THF ( $\tau = 0.64$  ns). Decays around 0.3 ns have been reported for polyfluorenes in solid state, which leads to the conclusion that the faster component may be associated with the polymer segments undergoing some type of quenching process in the condensed phase. Furthermore, we also observed that for longer wavelengths ( $\lambda_{\text{em}} = 460, 480$ , and 520 nm), an additional slower component appeared and a third component is required for a good fitting of the emission decay curve. When the decay is collected at  $\lambda_{\text{em}} = 520$  nm, there is a slower component with  $\tau_3 = 2.205$  ns and a contribution of  $B_3 = 43\%$ . It is reported in the literature that the fluorenone lifetimes were around 3–5 ns.<sup>31</sup> In conclusion, the emission decays also showed that, at least, two emitting species are present in the PFOFPe matrix: isolated chains and some other species which can be aggregates, fluorenone groups, or aggregated fluorenones.

As well-known, time-resolved emission spectroscopy (TRES) is a technique which shows the evolution of the spectra and how different emissions arise. In the present work, two different excitation wavelengths were used:  $\lambda_{\text{exc}} = 370$  nm for preferential

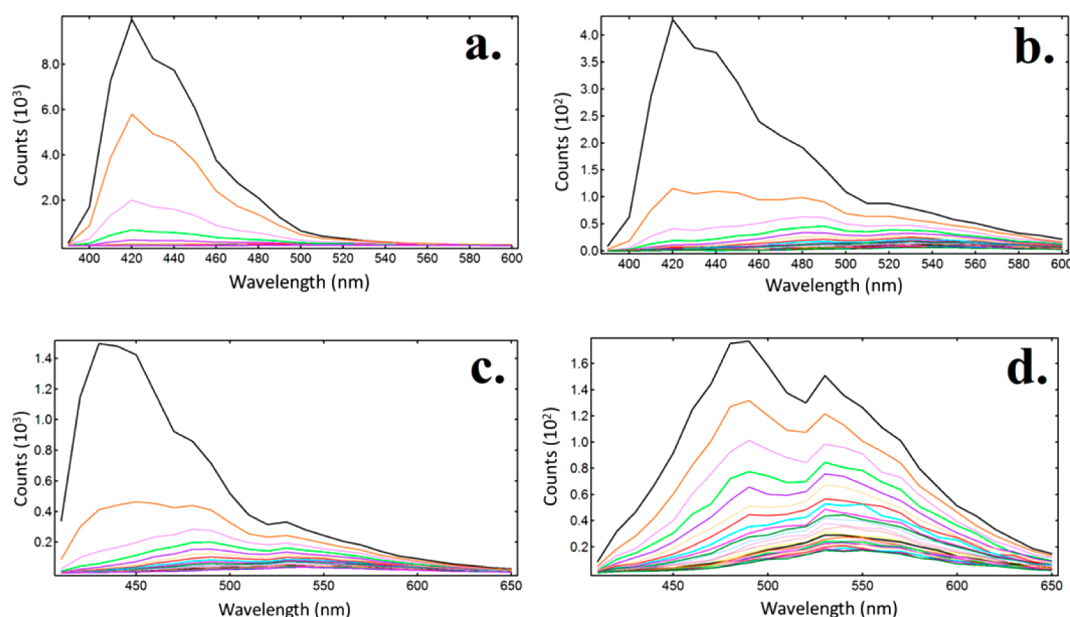


**Figure 7.** Time-resolved emission spectra (TRES) of PFOFPen spin-coated films obtained using (a and b)  $\lambda_{\text{exc}} = 370$  nm and  $\lambda_{\text{em}} = 410$ –620 nm and (c and d)  $\lambda_{\text{exc}} = 404$  nm and  $\lambda_{\text{em}} = 450$ –620 nm. The delays were (a and c) 0–4.5 ns and (b and d) 4.5–6.4 ns after the excitation pulses.

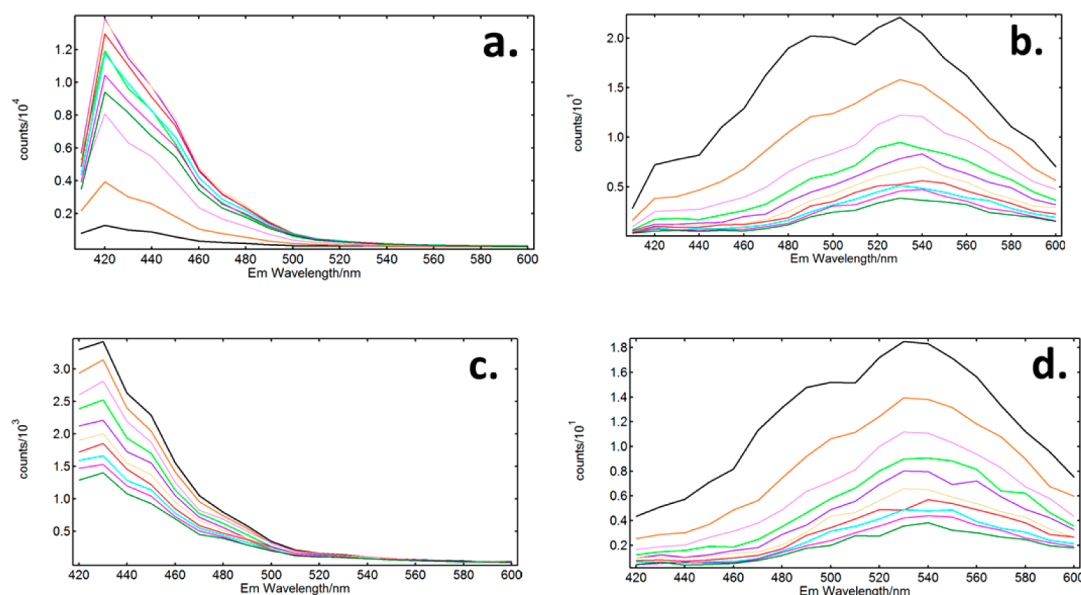


**Figure 8.** Time-resolved emission spectra (TRES) of PVK/PFOFPen spin-coated films obtained using (a and b)  $\lambda_{\text{exc}} = 370$  nm and  $\lambda_{\text{em}} = 410$ –620 nm and (c and d)  $\lambda_{\text{exc}} = 404$  nm and  $\lambda_{\text{em}} = 450$ –620 nm. The delays were (a and c) 0–4.5 ns and (b and d) 4.5–6.4 ns after the excitation pulses.

excitation of isolated chain segments (Figures 7, panels a and b) and  $\lambda_{\text{exc}} = 404$  nm for preferential excitation of the aggregated phase or the fluorenone groups (Figure 7, panels c and d). No emission has been observed when the excitation wavelengths are longer than 440 nm (data not shown). The emission band that is evident in the TRES spectrum presented in Figure 7a ( $\lambda_{\text{exc}} = 370$  nm and  $\lambda_{\text{em}} = 420$ –520 nm, shorter pulse delays) is essentially equivalent to that observed in steady-state PL spectrum with a PL band at higher energy (Figure 2a). The profile of this band is independent of the delay after the excitation pulse. Nevertheless a lower energy band appears for longer delays (Figure 7b) but always with a very low relative intensity. For excitation using 404 nm, the emission of isolated chains also predominates for shorter delays (Figure 7c), demonstrating that some nonaggregated chains are absorbing

and emitting. The green emission also appeared (with low intensity), indicating that the aggregates/defects are also emitting (Figure 7c). Moreover, for longer delays (Figure 7d), the green emission predominates, with a peak around 480 nm and a shoulder also appeared at 540 nm. This demonstrated that all types of lumophores were simultaneously excited when  $\lambda_{\text{exc}} = 404$  nm was used. Also, it is noteworthy that the emission profile of this band is not coincident with the EL emission of the green emitting species (Figure 2a).

A similar study was performed with the sample deposited on the PVK substrate, the same system as that used for the diode ITO/PEDOT:PSS/PVK/PFOFPen/Ca/Al, in which it was supposed that the PFOFPen was disaggregated by the PVK polymer (Figure 8). Again, both excitation wavelengths were used at  $\lambda_{\text{exc}} = 370$  nm and  $\lambda_{\text{exc}} = 404$  nm, and the TRES spectra

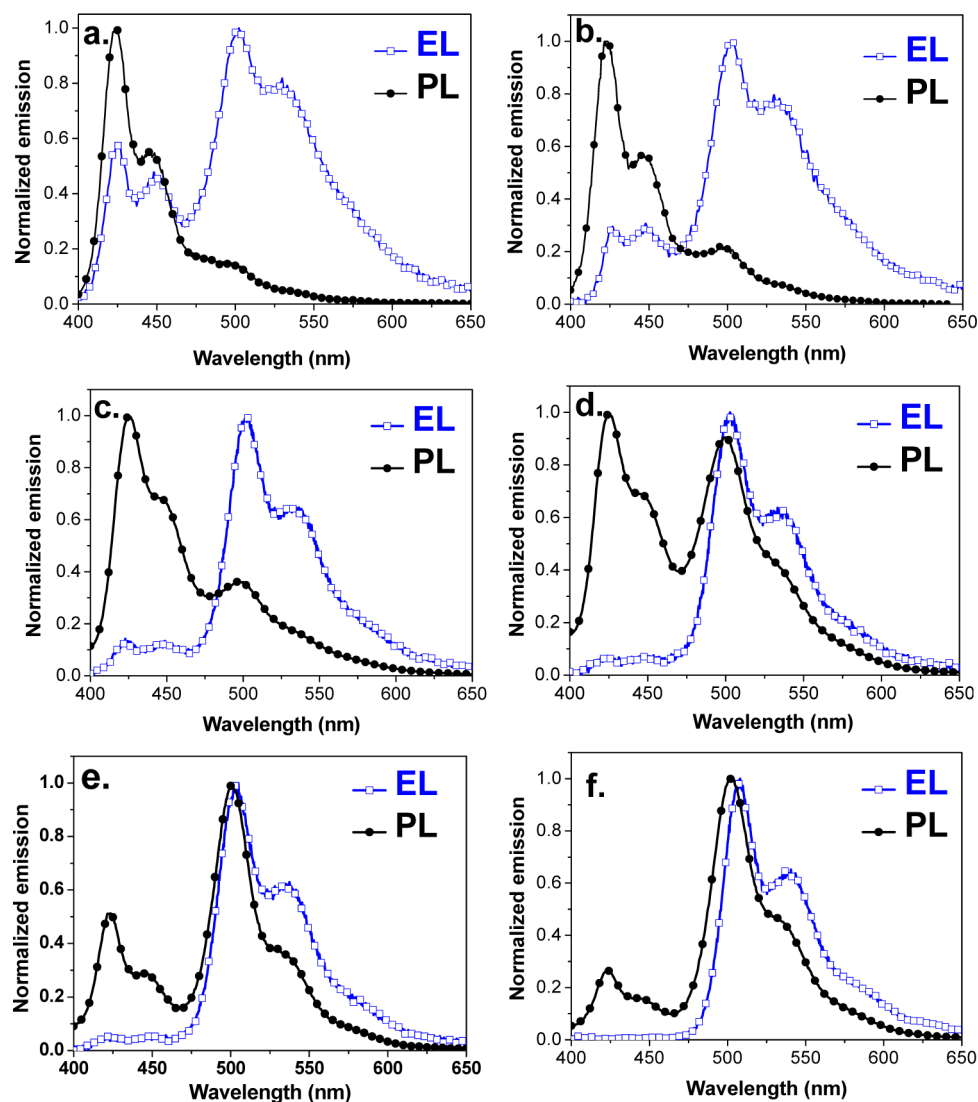


**Figure 9.** Comparison between the PL ( $\lambda_{\text{exc}} = 310$  nm) and EL spectra of polymer blends with various compositions of F6T2: (a) 0.0015, (b) 0.0075, (c) 0.075, (d) 0.37, (e) 0.75, and (f) 2.4 wt %. Device configuration: ITO/PEDOT:PSS(30 nm)/blend/Ca(30 nm)/Al(100 nm).

were recorded at several delays after the excitation pulse. For shorter delays (Figure 8, panels a and c), the spectral profiles are very similar for both excitation wavelengths and are also similar to that in absence of PVK (Figure 7, panels a and c). When using the excitation of 370 or 404 nm, the emission of the isolated groups is practically absent for longer delays (Figure 8, panels b and d), the higher intensity band is centered around 530 nm, and the band profile is different than that in the absence of PVK (Figure 7d). Thus, as indicated previously, the role of PVK induces polyfluorene disaggregation chains, but no influence on the fluorenone amount is expected.

Furthermore, our previous work regarding the attachment of the PFOFPen to polysiloxane chains showed that this green emission depends on the relative amount of both components.<sup>47</sup> Only for those samples with a greater amount of PFOFPen and with a greater relative ratio of attachment exhibited green emission. The conclusion of that work is that the green emission requires some kind of aggregated species of the PFOFPen. However, that study does not tell us what kind of aggregate is formed and also no information regarding to the presence of fluorenone moieties was presented.

Putting all of these spectroscopic data together, one can conclude that the fluorenone groups in the PFOFPen samples are very low (below the limit to be detected by the FTIR and <sup>13</sup>CNMR spectra), but some of their fingerprints appeared in both the emission decay at longer wavelengths and in the TRES when 404 nm is used for excitation. The more clear evidence for that is obtained when PFOFPen is in the presence of PVK, which disaggregates the polyfluorene. On the contrary, aggregates are evidenced when the TRES spectra of the PFOFPen is compared in the absence (Figure 7d) and presence of PVK (Figure 8d) the PFOFPen.

**3.3. EL and Electrical Properties of Diodes Fabricated Using PFOFPen/F6T2 Blends.** Figure 9 presents a comparison of the EL and PL emissions of diodes fabricated using PFOFPen/F6T2 blends with various concentrations of F6T2 (0.0015–2.4 wt %). Significant differences in band intensities between the EL and PL spectra of these blends were observed for different amounts of F6T2. The relative intensity of the two bands differs between the PL and EL spectra, and it can be described by the following ratio:



$$I_{\text{em}}^{\text{R}} = \frac{I_{\text{EL or PL}}(422 \text{ nm})}{I_{\text{EL or PL}}(505 \text{ nm})}$$

At lower concentrations of F6T2 (in the range of 0.0075–0.0015 wt %), both polymers emit in both the PL and EL spectra (Figure 9, panels a and b), with one band in the blue region and one in the green region. Table 2 summarizes the EL

**Table 2. Some Electrical Properties of Diodes with the Structure ITO/PEDOT:PSS(30 nm)/blend/Ca(30 nm)/Al(100 nm).  $I_{\text{em}}^{\text{R}}$  (PL) and  $I_{\text{em}}^{\text{R}}$  (EL) are the relative intensities of the band at 422 nm with respect to the band at 505 nm in the PL and EL spectra, respectively**

F6T2 (wt %)	$I_{\text{em}}^{\text{R}}$ (PL)	$I_{\text{em}}^{\text{R}}$ (EL)	$V_{\text{on}}$ (V)	$L_{\text{max}}$ (cd m <sup>-2</sup> )	$\text{CE}_{\text{max}}$ (cd A <sup>-1</sup> )	CIE (x, y)
0.0015	7.1	0.6	4.0	99	291	0.23, 0.39
0.0075	4.3	0.3	4.0	103	332	0.25, 0.46
0.075	2.7	0.1	3.6	137	761	0.24, 0.52
0.37	1.1	0.07	3.8	132	660	0.24, 0.55
0.75	0.5	0.0	3.8	156	503	0.24, 0.57
2.4	0.3	0.0	3.4	168	400	0.28, 0.62

$V_{\text{on}}$  = turn-on voltage,  $L_{\text{max}}$  = maximum luminance, and  $\text{CE}_{\text{max}}$  = maximum current efficiency. The CIE coordinates were obtained at 8 V.

characteristics and color coordinates (Figure 4) of these two diodes. However, the relative intensities of the two bands are substantially different between the two spectra. The most likely reason for this difference is that the amount of F6T2 is small, and therefore, the green emission in the PL spectrum is very low. On the contrary in the EL, the relative intensity of the F6T2 increases in comparison with the PFOFPe either because the HOMO and LUMO levels lied within PFOFPe band gap or because the F6T2 disaggregates the polyfluorene chains, as does the PVK.

The PL spectra of the 0.075 and 0.37 wt % blends also exhibit emission bands in the blue and green regions attributable to contributions from PFOFPe and F6T2, respectively (Figure 9, panels c and d). Nevertheless, the EL spectra essentially exhibit only the emission of the F6T2 copolymer. The PL relative intensity drops from 2.7 for 0.075 wt % F6T2 to 0.5 for 0.75 wt % F6T2 (Table 2), whereas the EL emission drops from 0.1 to 0.0 over the same concentration range. Even for 2.4 wt % F6T2, the PL spectrum (Figure 9f) exhibits emission bands (with low intensities) in the blue region (420–460 nm), although they disappear in the EL spectrum. For an F6T2 concentration of 2.4 wt %, the isolated chains of PFOFPe are completely quenched by F6T2 in the EL emission. For this diode, the CIE coordinates are (0.28, 0.62), which corresponds to the green region (Table 2). In terms of profile and position of the bands, the TRES measures of the PFOFPe/F6T2 blends (see Figure S4 of the Supporting Information) were very similar to the PL steady-state spectra.

There are two possibilities for the decrease of the EL emission intensity of the PFOFPe in the presence of the F6T2. One is the possibility of the resonant energy transfer process from the PFOFPe in the electronic excited state (the donor) to the F6T2 (the acceptor). The requirement for the FRET process from refs 45 and 46 is the spectral overlap between the emission band of the donor and the absorption band of the acceptor.<sup>45,46</sup> These two polymers exhibit a strong spectral overlap (see Figure S5 of the Supporting Information),

and this might be the reason for the spectral quenching observed in the PFOFPe emission in the blends. Nevertheless, if this is the only process playing a role in the EL devices, the relative intensities of the PFOFPe and F6T2 emissions should be the same in both EL and PL spectra. Thus, for EL, some other process might be contributing to the absence of the PFOFPe emission in the lowest concentration than in the PL. The hypothesis that can be postulated is the cascade mechanism for the charge injection<sup>15,16</sup> that favors the exciton formation in the polymer with lower energy gap, as one can see in the diagram with the frontier energy levels determined by cyclic voltammetry (Figure 10). The oxidation and reduction

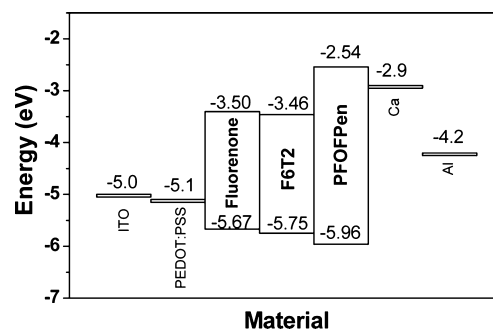


**Figure 10.** Diagram with the frontier energy levels of the PFOFPe and F6T2 determined by cyclic voltammetry. Values for the other components (ITO, Ca, PEDOT:PSS, and fluorenone) are from the literature.<sup>16,65</sup>

potentials for both polymers gave values for the highest occupied molecular orbital (HOMO) and the lowest unoccupied molecular orbital (LUMO) of −5.96 eV and −2.54 eV for PFOFPe and −5.75 eV and −3.07 eV for F6T2 (Figure 10). In accordance with the frontier energy levels of both materials, there is a greater probability of the exciton formation in the F6T2 by a cascade mechanism,<sup>16</sup> since the energy levels of the F6T2 lie within the band gap of the PFOFPe.

Figure 11 presents the electrical performance of these ITO/PEDOT:PSS(30 nm)/blends/Ca(30 nm)/Al(100 nm) diodes. In general, these devices exhibit typical diode behavior, and both the current density and the luminance increase sharply with voltage. The electrical properties depend on the blend composition. For example, for an applied voltage of 3.2 V, the luminance of the 2.4 wt % blend is brighter than that of pure PFOFPe (Table 2); the luminance and turn-on voltage decrease, and the efficiency increases with increasing F6T2 content. The CIE diagram (Figure 4) indicates that the color of the emission can be gradually tuned from blue to green as the F6T2 concentration increases from 0.0015 wt % to 2.4 wt %. It is quite impressive that such a remarkable color change can be achieved using such small amounts of the F6T2 component; this finding demonstrates that the F6T2 content has a much greater influence on the EL spectrum than on the PL spectrum in this regard.

## 4. CONCLUSIONS

The results presented here demonstrate that the emission color, as characterized by the CIE color coordinates of the EL spectrum, of a combination of the two investigated polymers can be gradually tuned. It was also demonstrated that the EL and PL emissions are nonequivalent in terms of the relative

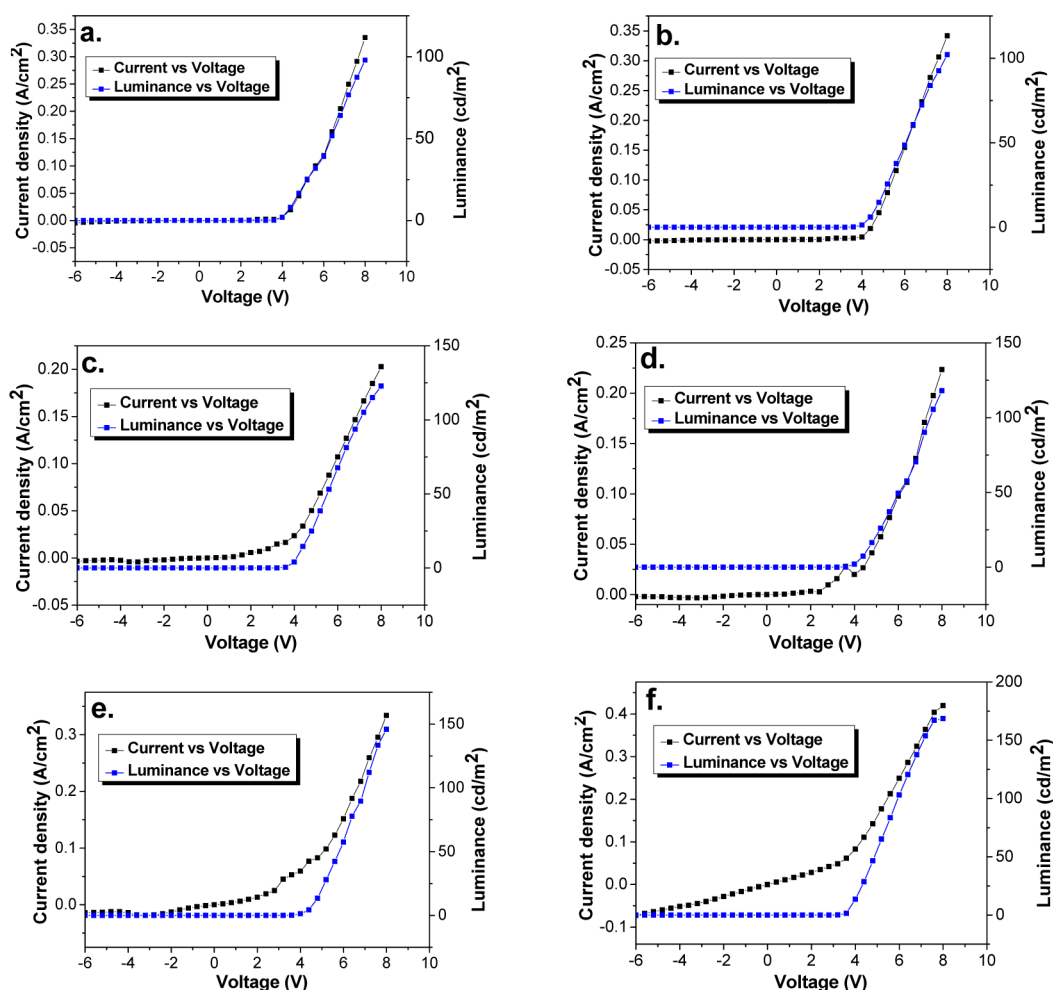


**Figure 11.** Current density vs voltage and luminance vs voltage graphs for ITO/PEDOT:PSS(30 nm)/blend/Ca(30 nm)/Al(100 nm) diodes fabricated using blends with various F6T2 contents: (a) 0.0015 wt %, (b) 0.0075 wt %, (c) 0.075 wt %, (d) 0.37 wt %, (e) 0.75 wt %, and (f) 2.4 wt %.

intensities of the two emission components; however, they are similar in terms of their spectral energies. It was demonstrated that the primary requirement for color tuning during the formation of the polymer blends is to ensure a suitable composition to avoid the complete quenching of the higher-energy component of the emission. The final color, as indicated by the CIE coordinates, can not be determined from the PL information. Furthermore, when one of the components of the polymer blend undergoes aggregation, which also leads to emission, the relative intensities in the EL and PL spectra might be very different because the exciton-formation efficiencies are different near isolated and aggregated chains. Some spectral evidence claiming the aggregates emission of the polyfluorene aggregates were demonstrated using a comparison of the samples with and without PVK, which disaggregates the polyfluorene chains. When aggregated, two emission bands are clearly observed in addition to the emission which should be associated with the fluorenone. The TRES spectra showed the aggregates emitting around 480 nm and the fluorenone around 520 nm. Comparing the EL emission of the PFOFPen in the absence and the presence of PVK lead us to conclude that aggregates are responsible by the green emission since no further oxidation process is evident during the diode operation. In this particular case, because the exciton-formation efficiency is higher in more ordered phases, the relative intensities of the

EL emission of such phases are also higher. Steady-state and dynamic photoluminescence techniques are useful methods for gaining insight into aggregation and aggregate emissions.

## ■ ASSOCIATED CONTENT

### § Supporting Information

<sup>13</sup>C NMR (Figure S1) and FTIR (Figure S2) spectra, emission decay curves of the PFOFPen (Figure S3) collected at different wavelengths, time-resolved emission spectra (TRES) of the PFOFPen/F6T2 blends (Figure S4), and the spectral overlap between PFOFPen emission and F6T2 absorption (Figure S5). This material is available free of charge via the Internet at <http://pubs.acs.org>.

## ■ AUTHOR INFORMATION

### Corresponding Author

\*E-mail: [tatvars@iqm.unicamp.br](mailto:tatvars@iqm.unicamp.br). Tel: +55-19-35214719.

### Notes

The authors declare no competing financial interest.

## ■ ACKNOWLEDGMENTS

The authors acknowledge FAPESP (Grants 2012-23460-4 and 2013/16245-2), CNPq, the National Institute of Organic

Electronics (INEO) (MCT/CNPq/FAPESP) and UNICAMP/FAEPEX for financial support and fellowships.

## REFERENCES

- (1) Burroughes, H. J.; Bradley, D. D. C.; Brown, A. R.; Marks, R. N.; Mackay, K.; Friend, R. H.; Burns, P. L.; Holmes, A. B. Light-Emitting Diodes Based on Conjugated Polymers. *Nature* **1990**, *347*, 539–541.
- (2) Friend, R. H.; Gymer, R. W.; Holmes, A. B.; Burroughes, J. H.; Marks, R. N.; Taliani, C.; Bradley, D. D. C.; Dos Santos, A. D.; Brédas, J. L.; Lögdlund, M.; et al. Electroluminescence in Conjugated Polymers. *Nature* **1999**, *397*, 121–128.
- (3) Nicolai, H. T.; Hof, A.; Blom, P. W. M. Device Physics of White Polymer Light-Emitting Diodes. *Adv. Funct. Mater.* **2012**, *22*, 2040–2047.
- (4) Joo, C. W.; Jeon, S. O.; Yook, K. S.; Lee, J. Y. Multilayer Stacked White Polymer Light-Emitting Diodes. *J. Phys. D: Appl. Phys.* **2009**, *42*, 105115.
- (5) Reineke, S.; Thomschke, M.; Lüssem, B.; Leo, K. White Organic Light-Emitting Diodes: Status and Perspectives. *Rev. Phys. Mod.* **2013**, *85*, 1245.
- (6) Schubert, E. F.; Kim, J. K. Solid-State Light Sources Getting Smart. *Science* **2005**, *308*, 1274–1278.
- (7) *Organic Light-Emitting Devices: A Survey*; Shinar, J., Ed.; Springer-Verlag: New York, 2004.
- (8) Gather, M. C.; Köhnen, A.; Meerholz, K. White Organic Light-Emitting Diodes. *Adv. Mater.* **2011**, *23*, 233–248.
- (9) Tash, B.; Brandstätter, C.; Meghdadi, F.; Leising, G.; Froyer, G.; Athouel, L. Red-Green-Blue Light Emission from a Thin Film Electroluminescence Device Based on Parahexaphenyl. *Adv. Mater.* **1997**, *9*, 33–36.
- (10) Amin, G.; Zaman, S.; Zainelabdin, A.; Nur, O.; Willander, M. ZnO Nanorods-Polymer Hybrid White Light Emitting Diode Grown on a Disposable Paper Substrate. *Phys. Status Solidi RRL* **2011**, *5*, 71–73.
- (11) Huang, F.; Wu, H.; Cao, Y. Water/Alcohol Soluble Conjugated Polymers as Highly Efficient Electron Transporting/Injection Layer in Optoelectronic Devices. *Chem. Soc. Rev.* **2010**, *39*, 2500–2521.
- (12) Sessolo, M.; Tordera, D.; Bolink, H. J. Ionic Iridium Complex and Conjugated Polymer Used to Solution Process a Bilayer White Light-Emitting Diode. *ACS Appl. Mater. Interfaces* **2013**, *5*, 630–634.
- (13) Tang, C.; Liu, X.-D.; Liu, F.; Wang, X.-L.; Xu, H.; Huang, W. Recent Progress in Polymer White Light-Emitting Materials and Devices. *Macromol. Chem. Phys.* **2013**, *214*, 314–342.
- (14) Zhu, M.; Zou, J.; Hu, S.; Li, C.; Yang, C.; Wu, H.; Qin, J.; Cao, Y. Highly Efficient Single-Layer White Polymer Light-Emitting Devices Employing Triphenylamine-based Iridium Dendritic Complexes as Orange Emissive Component. *J. Mater. Chem.* **2012**, *22*, 361–366.
- (15) de Deus, J. F.; Faria, G. C.; Faria, R. M.; Iamazaki, E. T.; Atvars, T. D. Z.; Cirpan, A.; Akcelrud, L. White Light Emitting Devices by Doping Polyfluorene with Two Red Emitters. *J. Photochem. Photobiol., A* **2013**, *253*, 45–51.
- (16) de Deus, J. F.; Faria, G. C.; Iamazaki, E. T.; Faria, R. M.; Atvars, T. D. Z.; Akcelrud, L. Polyfluorene Based Blends for White Light Emission. *Org. Electron.* **2011**, *12*, 1493–1504.
- (17) Liu, J.; Chen, Y.; Qin, D.; Cheng, C.; Quan, W.; Chen, L.; Li, G. Improved Interconnecting Structure for a Tandem Organic Light Emitting Diode. *Semicond. Sci. Technol.* **2011**, *26*, 095011.
- (18) Nowacki, B.; Grova, I. R.; Domingues, R. A.; Faria, G. C.; Atvars, T. D. Z.; Akcelrud, L. Photo- and Electroluminescence in a Series of PPV Type Terpolymers Containing Fluorene, Thiophene and Phenylene Units. *J. Photochem. Photobiol., A* **2012**, *237*, 71–79.
- (19) Ikawa, S.; Yagi, S.; Maeda, T.; Nakazumi, H. White Polymer Light-Emitting Diodes Co-Doped with Phosphorescent Iridium Complexes Bearing the Same Cyclometalated Ligand. *Phys. Status Solidi C* **2012**, *9*, 2553–2556.
- (20) Farinola, G. M.; Ragni, R. Electroluminescent Materials for White Organic Light Emitting Diodes. *Chem. Soc. Rev.* **2011**, *40*, 3467–3482.
- (21) Huang, C.-Y.; Huang, T.-S.; Cheng, C.-Y.; Chen, Y.-C.; Wan, C.-T.; Rao, M. V. M.; Su, Y.-K. Three-Band White Light-Emitting Diodes Based on Hybridization of Polyfluorene and Colloidal CdSe-ZnS Quantum Dots. *IEEE Photonics Technol. Lett.* **2010**, *22*, 305–307.
- (22) Kang, B.-H.; You, T.-Y.; Yeom, S.-H.; Kim, K.-J.; Kim, S.-H.; Lee, S.-W.; Yuan, H.; Kwon, D.-H.; Kang, S.-W. Highly Efficient White Light-Emitting Diodes Based on Quantum Dots and Polymer Interface. *IEEE Photonics Technol. Lett.* **2012**, *24*, 1594–1596.
- (23) Dawson, K.; Lovera, P.; Iacopino, D.; O’Riordan, A.; Redmond, G. Multi-Colour Emission from Dye Doped Polymeric Nanotubes by Host-Guest Energy Transfer. *J. Mater. Chem.* **2011**, *21*, 15995–16000.
- (24) Ye, T.; Chen, J.; Ma, D. Electroluminescence of Poly(N-vinylcarbazole) Films: Fluorescence, Phosphorescence and Electromers. *Phys. Chem. Chem. Phys.* **2010**, *12*, 15410–15413.
- (25) Cheng, Y.-J.; Liao, M.-H.; Shih, H.-M.; Shih, P.-I.; Hsu, C.-S. Exciplex Electroluminescence Induced by Cross-linked Hole-transporting Materials for White Light Polymer Light-Emitting Diodes. *Macromolecules* **2011**, *44*, S968–S976.
- (26) Baek, S. J.; Chang, H. J. Fabrication and Characterization of White Polymer Light Emitting Diodes using PFO:MDMO-PPV. *J. Nanosci. Nanotechnol.* **2012**, *12*, 3606–3610.
- (27) Akcelrud, L. Electroluminescent polymers. *Prog. Polym. Sci.* **2003**, *28*, 875–962.
- (28) Huebner, C. F.; Foulger, S. H. Spectral Tuning of Conjugated Polymer Colloid Light-Emitting Diodes. *Langmuir* **2010**, *26*, 2945–2950.
- (29) Beaujuge, P. M.; Reynolds, J. R. Color Control in  $\pi$ -conjugated Organic Polymers for Use in Electrochromic Devices. *Chem. Rev.* **2010**, *110*, 268–320.
- (30) Nowacki, B.; Iamazaki, E.; Cirpan, A.; Karasz, F.; Atvars, T. D. Z.; Akcelrud, L. Highly Efficient Polymer Blends from a Polyfluorene Derivative and PVK for LEDs. *Polymer* **2009**, *50*, 6057–6064.
- (31) Kulkarni, A. P.; Jenekhe, S. A. Blue Light-Emitting Diodes with Good Spectral Stability Based on Blends of Poly(9,9-dioctylfluorene): Interplay between Morphology, Photophysics, and Device Performance. *Macromolecules* **2003**, *36*, 5285–5296.
- (32) Bernardo, G.; Charas, A.; Morgado, J. Luminescence Properties of Poly(9,9-dioctylfluorene)/Polyvinylcarbazole Blends: Role of Composition on the Emission Colour Stability and Electroluminescence Efficiency. *J. Phys. Chem. Solids* **2010**, *71*, 340–345.
- (33) Arias, A. C.; Mackenzie, J. D.; McCulloch, I.; Rivnay, J.; Salleo, A. Materials and Applications for Large Area Electronics: Solution-based Approaches. *Chem. Rev.* **2010**, *110*, 3–24.
- (34) Zhou, Y.; Fuentes-Hernandez, C.; Khan, T. M.; Liu, J.-C.; Hsu, J.; Shim, J. W.; Dindar, A.; Youngblood, J. P.; Moon, R. J.; Kippelen, B. Recyclable Organic Solar Cells on Cellulose Nanocrystal Substrates. *Sci. Rep.* **2013**, *3*, 1536.
- (35) Paul, D. R.; Barlow, J. W. A Binary Interaction Model for Miscibility of Copolymers in Blends. *Polymer* **1984**, *25*, 487–497.
- (36) Stevens, A. L.; Kaeser, A.; Schenning, A. P. H. J.; Herz, L. M. Morphology-Dependent Energy Transfer Dynamics in Fluorene-based Amphiphile Nanoparticles. *ACS Nano* **2012**, *26*, 4777–4787.
- (37) Antony, M. J.; Jayakannan, M. Molecular Template Approach for Evolution of Conducting Polymer Nanostructures: Tracing the Role of Morphology on Conductivity and Solid State Ordering. *J. Phys. Chem. B* **2010**, *114*, 1314–1324.
- (38) Rogers, J. T.; Schmidt, K.; Toney, M. F.; Kramer, E. J.; Bazan, G. C. Structural Order in Bulk Heterojunction Films Prepared with Solvent Additives. *Adv. Mater.* **2011**, *23*, 2284–2288.
- (39) Chen, X.; Wan, H.; Li, H.; Cheng, F.; Yao, B.; Xie, Z.; Wang, L.; Zhang, J. Influence of Thermal Annealing Temperature on Electro-optical Properties of Polyoctylfluorene Thin Film: Enhancement of Luminescence by Self-doping Effect of Low-content  $\alpha$  Phase Crystallites. *Polymer* **2012**, *53*, 3827–3832.
- (40) Garcia, A.; Welch, G. C.; Ratcliff, E. L.; Ginley, D. S.; Bazan, G. C.; Olson, D. C. Improvement of Interfacial Contacts for New Small-Molecule Bulk-Heterojunction Organic Photovoltaics. *Adv. Mater.* **2012**, *24*, S368–S373.



- (41) Clark, J.; Silva, C.; Friend, R. H.; Spano, F. C. Role of Intermolecular Coupling in the Photophysics of Disordered Organic Semiconductors: Aggregate Emission in Regioregular Polythiophene. *Phys. Rev. Lett.* **2007**, *98*, 206406.
- (42) Noriega, R.; Rivnay, J.; Vandewal, K.; Koch, F. P. V.; Stingelin, N.; Smith, P.; Toney, M. F.; Salleo, A. A General Relationship between Disorder, Aggregation and Charge Transport in Conjugated Polymers. *Nat. Mater.* **2013**, *12*, 1038–1044.
- (43) Wood, S.; Kim, J. S.; James, D. T.; Tsoi, W. C.; Murphy, C. E.; Kim, J.-S. Understanding the Relationship between Molecular Order and Charge Transport Properties in Conjugated Polymer Based Organic Blend Photovoltaic Devices. *J. Chem. Phys.* **2013**, *139*, 064901.
- (44) Sahoo, H. Förster Resonance Energy Transfer: A Spectroscopic Nanoruler: Principle and Applications. *J. Photochem. Photobiol., C* **2011**, *12*, 20–30.
- (45) Förster, Th. 10TH Spiers Memorial Lecture Transfer Mechanisms of Electronic Excitation. *Discuss. Faraday Soc.* **1959**, *27*, 7–17.
- (46) Glossary of terms used in Photochemistry. 3rd edition (IUPAC Recommendations 2006). *Pure Appl. Chem.* **2007**, *79*, 293–465.
- (47) Quites, F. J.; Domingues, R. A.; Ferbonick, G. F.; Nome, R. A.; Atvars, T. D. Z. Facile Control of System-bath Interactions and the Formation of Crystalline Phases of Poly[(9,9-dioctylfluorenyl-2,7-diyl)-alt-co-(9,9-di-{50-pentanyl}-fluorenyl-2,7-diyl)] in Silicone-Based Polymer Hosts. *Eur. Polym. J.* **2013**, *3*, 693–705.
- (48) Gadermaier, C.; Luer, L.; Gambetta, A.; Virgili, T.; Zavelani-Rossi, M.; Lanzani, G.; Hadziioannou, G.; Malliaras, G. G. Photo-physics in Semiconducting Polymers: The Case of Polyfluorenes. *Semicond. Polym.* (2nd Ed.) **2007**, *1*, 205–234.
- (49) Chunwaschirasiri, W.; Tanto, B.; Huber, D. L.; Winokur, M. J. Chain Conformations and Photoluminescence of Poly(di-n-octylfluorene). *Phys. Rev. Lett.* **2005**, *94*, 107402.
- (50) Bright, D. W.; Galbrecht, F.; Scherf, U.; Monkman, A. P.  $\beta$  Phase Formation in Poly(9,9-di-n-decylfluorene). Thin Films. *Macromolecules* **2010**, *43*, 7860–7893.
- (51) O'Carroll, D.; Iacopino, D.; O'Riordan, A.; Lovera, P.; O'Connor, E.; O'Brien, G. A.; Redmond, G. Poly(9,9-dioctylfluorene) Nanowires with Pronounced  $\beta$ -phase Morphology: Synthesis, Characterization, and Optical Properties. *Adv. Mater.* **2008**, *20*, 42–48.
- (52) Sergeant, A.; Zucchi, G.; Pansu, R. B.; Chaigneau, M.; Geffroy, B.; Tondelier, D.; Ephritikhine, M. Synthesis, Characterization, Morphological Behavior, and Photo- and Electroluminescence of Highly Blue-Emitting Fluorene-Carbazole Copolymers with Alkyl Side-Chains of Different Lengths. *J. Mater. Chem. C* **2013**, *1*, 3207–3216.
- (53) Grimsdale, A. C.; Müller, K. Bridged Polyphenylenes: From Polyfluorenes to Ladder Polymers. *Adv. Polym. Sci.* **2008**, *212*, 1–48.
- (54) Ananthakrishnan, S. J.; Varathan, E.; Ravindran, E.; Somanathan, N.; Subramanian, V.; Mandal, A. B.; Sudhac, J. D.; Ramakrishnan, R. A. A solution processable Fluorine-Fluorenone Oligomer with Aggregation Induced Emission Enhancement. *Chem. Commun.* **2013**, *49*, 10742–10744.
- (55) Sun, Q. J.; Fan, B. H.; Tan, Z. A.; Yang, C. H.; Lia, Y. F.; Yang, Y. White light from Polymer Light-Emitting Diodes: Utilization of Fluorenone Defects and Exciplex. *Appl. Phys. Lett.* **2006**, *88*, 163510.
- (56) Jenekhe, S. A.; Osaheni, J. A. Excimers and Exciplexes of Conjugated Polymers. *Science* **1994**, *265*, 765–768.
- (57) Yu, W. L.; Pei, J.; Huang, W.; Heeger, A. S. Spiro-Functionalized Polyfluorene Derivatives as Blue Light-Emitting Materials. *Adv. Mater.* **2000**, *12*, 828–831.
- (58) Bliznyuk, V. N.; Carter, S. A.; Scott, J. C.; Kramer, G.; Miller, R. D.; Miller, D. G. *Macromolecules* **1999**, *32*, 361.
- (59) Zhao, W.; Cao, T.; White, J. M. On the Origin of Green Emission in Polyfluorene Polymers: The Roles of Thermal Oxidation Degradation and Crosslinking. *Adv. Funct. Mater.* **2004**, *14*, 783–790.
- (60) Zhang, M.-S.; Wang, D.-E.; Xue, P.; Wang, W.; Wang, J.-C.; Tu, Q.; Liu, Z.; Liu, Y.; Zhang, Y.; Wang, J. Fluorenone Organic Crystals: Two-Color Luminescence Switching and Reversible Phase Transformations between  $\pi$ - $\pi$  Stacking-Directed Packing and Hydrogen Bond-Directed Packing. *Chem. Mater.* **2014**, *26*, 2467–2477.
- (61) Grisorio, R.; Allegretta, G.; Mastrorilli, P.; Suranna, G. P. On the Degradation Process Involving Polyfluorenes and the Factors Governing Their Spectral Stability. *Macromolecules* **2011**, *44*, 7977–7986.
- (62) Kwon, Y. K.; Kim, H. S.; Kim, H. J.; Oh, J. H.; Park, H. S.; Ko, Y. S.; Kim, K. B.; Kim, M. S. Reduced Excimer Formation in Polyfluorenes by Introducing Coil-like Poly[penta(ethylene glycol) methyl ether methacrylate] Block Segments. *Macromolecules* **2009**, *42*, 887–891.
- (63) Tozoni, J. R.; Guimarães, F. G.; Atvars, T. D. Z.; Nowacki, B.; Marletta, A.; Akcelrud, L.; Bonagamba, T. J. De-Aggregation of Polyfluorene Derivative by Blending with a Series of Poly(alkyl methacrylate)s with Varying Side Group Sizes. *Eur. Polym. J.* **2009**, *45*, 2467–2477.
- (64) Chakraborty, C.; Dana, K.; Malik, S. Immobilization of Poly(fluorene) within Clay Nanocomposite: An Easy Way to Control Keto Defect. *J. Colloid Interface Sci.* **2012**, *368*, 172–180.
- (65) Kuik, M.; Wetzelaer, G.-J.A.H.; Laddé, J. G.; Nicolai, H. T.; Wildeman, J.; Sweelssen, J.; Bloom, P. W. M. The Effect of Ketone Defects on the Charge Transport and Charge Recombination in Polyfluorenes. *Adv. Funct. Mater.* **2011**, *21*, 4502–4509.
- (66) Lee, J. I.; Klaemer, G.; Miller, R. D. Oxidative Stability and Its Effect on the Photoluminescence of Poly(fluorene) Derivatives: End Group Effects. *Chem. Mater.* **1999**, *11*, 1083–1088.
- (67) List, W. E. J.; Guentner, R.; de Freitas, P. S.; Scherf, U. The Effect of Keto Defect Sites on the Emission Properties of Polyfluorene-Type Materials. *Adv. Mater.* **2002**, *14*, 374–378.
- (68) Yang, G.-Z.; Wu, M.; Lu, S.; Wang, M.; Liu, T.; Huang, W. Thermooxidative Stability of Spectra of Fluorene-based Copolymers. *Polymer* **2006**, *47*, 4816–4823.
- (69) Uckert, F.; Setayesh, S.; Müllen, K. A Precursor Route to 2,7-Poly(9-fluorenone). *Macromolecules* **1999**, *32*, 4519–4524.